MECHANICAL PROPERTIES – TRANSLUCENCY - MICROSTRUCTURE RELATIONSHIPS IN COMMERCIAL MONOLAYER AND MULTILAYER MONOLITHIC ZIRCONIA CERAMICS

Stevan M. Čokić[1], Mar Cóndor[3], Jef Vleugels[2], Bart Van Meerbeek[1], Hans Van Oosterwyck[3], Masanao Inokoshi[4], Fei Zhang[1,2]

[1]KU Leuven (University of Leuven), Department of Oral Health Sciences, BIOMAT & UZ Leuven (University Hospitals Leuven), Dentistry, Leuven, Belgium;

[2]KU Leuven (University of Leuven), Department of Materials Engineering (MTM), Kasteelpark Arenberg 44, B-3001, Leuven, Belgium;

[3]KU Leuven (University of Leuven), Department of Mechanical Engineering, Biomechanics Section (BMe), Arenberg, Leuven, Belgium;

[4]Department of Gerodontology and Oral Rehabilitation, Graduate School of Medical and Dental Sciences, Tokyo Medical and Dental University, 1-5-45 Yushima, Bunkyo, Tokyo 113-8549, Japan;

Corresponding author: Dr. Stevan Čokić, KU Leuven (University of Leuven), Department of Oral Health Sciences, BIOMAT, Kapucijnenvoer 7, blok a – box 7001, BE-3000 Leuven, Belgium. TEL: +32-16-373394, FAX: +32-16-373394, stevan.cokic@kuleuven.be

Key words: Monolithic zirconia; Multilayer zirconia; Mechanical properties; Finite Element Analysis, Parameter analysis

Declarations of interest

Declarations of interest: none.

HIGHLIGHTS

- FEA validated the equations to calculate the biaxial strength when testing plate-shape specimens
- 3Y-TZP and 4Y-PSZ ceramics showed the highest fracture toughness and flexural strength as compared to other zirconia grades
- 3Y-TZP ceramics had lower mechanical reliability than 4Y-PSZ but were more reliable than 5Y-PSZ and 6Y-PSZ ceramics
- 6Y-PSZ and 5Y-PSZ zirconia grades had a higher translucency than the opaquer 4Y-PSZ and 3Y-TZP zirconia grades

ABSTRACT

Objectives: To evaluate the phase composition, microstructure, optical properties and mechanical properties of eight commercially available multilayer and monolayer monolithic dental zirconias.

Methods: Five commercial 3Y-TZP (GC ST, GC HT [GC, Tokyo Japan]; Katana ML, Katana HT [Kuraray Noritake] and Lava Plus [3M Oral Care]) and three Y-PSZ (Katana STML, Katana UTML [Kuraray Noritake]; GC UHT [GC, Tokyo Japan]) zirconia ceramic grades were cut in plate-shaped specimens, sintered according to the manufacturer's instructions and mirror polished. The zirconia chemical composition was determined using X-ray fluorescence (XRF), phase composition was characterized using X-ray diffraction (XRD), while the grain size was measured using scanning electron microscopy (SEM). The translucency Parameter (TP) and Contrast Ratio (CR) were measured with a spectrophotometer (n=10/group). The indentation fracture toughness (n=10), Vickers hardness (n=10) and biaxial strength (n=20) of the sintered ceramics were assessed. The stress distribution during biaxial testing was assessed by Finite element analysis (FEA). Statistical analysis involved one-way ANOVA and post-hoc Tukey's HSD test and Pearson correlation test (α=0.05).

Results: FEA showed that the stress distribution in plate shape specimens was the same as for disks, rationalizing the use of plates for biaxial strength testing. As expected, higher quantities of Y_2O_3 were related to a higher cubic ZrO_2 phase content and lower tetragonality t-ZrO_2, which improved translucency but diminished flexural strength and toughness. While there was no significant correlation between grain size and other material properties, addition of pigments to the zirconia grade statistically negatively affected hardness.

Conclusion: Even though an improvement in strength and translucency could be recorded for the last Y-TZP generation, future research still needs to strive for combined improvement of optical properties and mechanical reliability of zirconia ceramics.

1. INTRODUCTION

Since it was first marked as a high performing ceramic or so called “ceramic steel” by Garvie et al. in 1975 [1], zirconia-based materials have found their place in dentistry due to their superior biocompatibility, favorable mechanical properties and promising esthetic potential. So far, dental material manufacturers have, through 3 successive generations, designed and produced various types of zirconia dental ceramics distinguished by their composition, mechanical properties, translucency (low, medium, high, super and ultra) and shade (unstained, stained, multilayered) [2,3]. Chronologically, the first generation 3 mol% yttria stabilized zirconia (3Y-TZP) was designed with a high amount (≥0.25 wt%) of alumina (Al_2O_3) and is characterized by a combination of high strength (≈1000 MPa) and good fracture toughness (≈5 $MPa \cdot m^{1/2}$), but at the same time high opacity, which limited their use to long span fixed dental prostheses (FDPs) in the posterior load bearing areas. In order to improve their translucency and broaden their indications, a second generation of zirconia was developed, involving a drastic reduction of the alumina content (to 0.1 or 0.05 wt%) and elimination of porosity by sintering at higher temperature [3]. Even though some optical improvements were achieved, these zirconias were still insufficiently aesthetically appealing for the use in the anterior esthetic zone. The translucency of the third generation of zirconia was improved by additional doping of ZrO_2 powder with Y_2O_3 (> 4 mol%); it significantly increased the amount of non-birefringent cubic ZrO_2 phase at the expense of flexural strength and fracture toughness [4]. At present, the Y_2O_3 content, the concomitant tetragonal or cubic phase content and fracture toughness are determining and predicting parameters for clinical indications in dentistry [5].

Another parameter that is important for the clinical indication of dental zirconia is their primary color, as white to ivory does not resemble the natural color of teeth [6,7]. Recently, new multilayer zirconia ceramics have been manufactured by pressing various pigment-doped ZrO_2 layers, with the intention to accurately replicate the gradual color change from the cervical to the incisal part of the crown. However, added coloring agents can act as impurities in the sintered zirconia ceramics affecting microstructure, translucency and flexural strength [8]. Ban *et al.* reported that zirconia colored with Er^{3+} and Nd^{3+} ion containing liquid, resulted in a reduction of flexural strength and fracture toughness [9]. Moreover, Tuncel *et al.* (2013) revealed that specific coloring liquids can decrease the translucency of zirconia frameworks [10]. On the other hand, various research showed opposite results without significant correlation between colored zirconia and their mechanical properties [11,12]. It is clear that this correlation is not fully understood and additional research is highly warranted [8,9].

Various dental companies are specialized in the processing of powder into semi-final zirconia blanks and have developed different approaches and techniques, such as isostatic powder pressing or pre-sintering; they play a crucial role in the final quality of the pre-sintered zirconia blanks and subsequently final zirconia product. These various approaches are responsible for the large difference

between commercial products [13]. Numerous studies have already shown that a slight modification of the ZrO_2 starting powder composition can significantly influence the material microstructure and inevitably its mechanical strength, fracture toughness and long-term stability [14]. Additionally, the sintering parameters are also considered to be a critical step in ceramic processing and can directly influence the density and microstructure, including grain size and phase composition, which again can affect the mechanical and optical properties [15].

To the best of the authors' knowledge, information regarding a detailed evaluation of the broad spectra of commercially available zirconia ceramics, in particular the correlations between the physical (yttria content, phase composition, crystal lattice parameters, grain size), mechanical (toughness, hardness and strength) and optical properties (translucency and in particular color) is still missing. Therefore, the main objective of this study was to fill this gap by studying different generations of commercially available multi- and monolayer dental zirconia ceramics. Importantly, instead of using disks, as proposed in the ISO standard [16], plate-shaped specimens which are more relevant and compatible to the commercially available pre-sintered blocks especially for chairside treatment [17] are used for biaxial strength testing. Finite element analysis (FEA) was performed in order to determine the stress distributions during loading of a plate-shaped specimen in a piston-on-three-balls set-up (P3B). The null hypothesis of this study was that there is no relationship between specific physical, mechanical and optical properties of both monolayer and multilayer zirconia grades.

2. MATERIALS & METHODS

2.1. Commercial materials and specimen preparation

Eight commercial pre-sintered zirconia ceramics (Table 1: GC ST, GC HT and GC UHT, GC, Tokyo, Japan; Katana HT, Katana ML, Katana STML and Katana UTML, Kuraray Noritake, Tokyo, Japan; Lava Plus, 3M Oral Care, Seefeld, Germany) were cut into dimensions of approximate by 15 × 15 × 3.5 mm, 18 × 18 × 3.5 mm or 12 × 12 × 3.5 mm, depending on the thickness of the pre-sintered ceramic blank provided by the suppliers. All specimens were cut through whole ceramic pre-sintered disk in order to include all the layers in the analysis. Specimens were pressureless sintered in air according to the manufacturers' instructions (Table 1) using a computer-programmed furnace (Nabertherm, Lilienthal, Germany) reaching the final specimen dimensions of (1) ≈10 × 10 × 1.2 mm for GC ST and GC HT; (2) ≈12 x 12 x 1.2 mm for Katana HT, Katana ML, Katana STML, Katana UTML and Lava HT; (3) ≈15 × 15 × 1.2 mm for GC UHT. The sintered materials were ground plane parallel and gradually polished down to 1 µm with diamond suspensions and finally with colloidal silica until a mirror-glass surface was achieved. The final specimen thickness was 0.5 ± 0.05 mm for evaluating the microstructure and optical properties and 1.2 ± 0.05 mm for analyzing the biaxial flexural strength.

2.2. Characterization of physical properties: microstructure, chemical and phase compositions

The microstructural, chemical and phase features of different dental zirconia were thoroughly studied in order to elucidate their relationships with the optical and mechanical properties.

The microstructure was characterized using scanning electron microscopy (SEM; Philips XL-30 FEG, Eindhoven, The Netherlands). Sintered ceramics were mirror polished and thermally etched (1250 °C), and Pt coated to reveal the grain boundary network. Secondary electron (SE) images were acquired at 10^{-5} mbar pressure, an acceleration voltage of 10 kV and 144 µA beam current in random parts of the specimen including all layers of multilayered materials. The zirconia grain size of at least 1000 grains was measured on SE micrographs using Image-Pro PLUS 6.0 software (Media Cybernetics, Rockville Pike, USA) according to the linear intercept method [23]. The average grain size with standard deviation and grain-size distributions were reported without any corrections.

The chemical composition of the zirconia grades was evaluated by wavelength dispersive X-ray fluorescence spectroscopy (WD-XRF; Bruker S8 Tiger, Germany) using a 4 kW X-ray tube. Due to the large beam size, sampling of all materials was done from the center of the plate shaped specimens. In particular, to assess the contents of the Y_2O_3 stabilizer and other coloring additives, for which merely the ranges are provided by the manufacturers. The chemical composition in oxide wt% was calculated using build-in Quant-Express software (Bruker, Karlsruhe,Germany).

X-ray diffraction (XRD; 3003 T/T, Seifert, Ahrensburg, Germany) was performed to identify the phase composition. As-sintered surfaces of each material were scanned using Cu K_α (40 kV, 40 mA) irradiation from 20 to 90° 2θ with the step size of 0.01° for 3s. Specimen were analyzed at the center. Rietveld analysis was performed using TOPAS Academic V5 software (Coelho software, Brisbane, Australia) to determine the phase composition and lattice parameters of each zirconia grade. The Y_2O_3 content in the tetragonal ZrO_2 phase was calculated based on the *a* and *c* unit cell parameter of the tetragonal ZrO_2 phase, according to Yamashita *et al* (2005). and Gibson *et al.* (2001) [18,19]*:*

$$YO_{1.5}\,(mol\%) = \frac{1.0223 - \frac{c_t}{\sqrt{2}a_t}}{0.001319} \qquad (1)$$

µRaman spectra (SENTERRA, BrukerOptik, Ettlingen, Germany) were collected using an Ar-ion laser with a wavelength of 532 nm, 20 mW power at specimen and 20× objective (lateral resolution: ≤4 µm) and a pinhole aperture of 50 µm. The spectrum integration time was 20s with the recorded spectra averaged over three successive measurements. Six points were recorded for each analyzed specimen.

2.3. Optical property characterization

The translucency of the ceramics was determined on double-sided mirror-glass polished specimens (n=10, thickness of 0.5 mm) using a spectrophotometer (SpectroShadeTM MICRO, MHT Optic Research, Niederhasli, Switzerland). Lithium-disilicate glass-ceramic (LS_2) specimens (n=7, thickness of 0.5 mm) were prepared from an IPS e.max CAD HT block (Ivoclar Vivadent, Schaan, Liechtenstein; "HT" = high translucency) as a translucency reference control. The spectrometer was used to record the CIELAB coordinates (L*, a* and b*) of each ceramic disk positioned on a black and white background. A thin layer of vaseline was put in between specimen and background for better optical contact. The translucency parameter (TP) was calculated according to:

$$TP = \sqrt{(L_B^* - L_W^*)^2 + (a_B^* - a_W^*)^2 + (b_B^* - B_W^*)^2} \quad (2)$$

where the subscripts B and W refer to the color coordinates over a black and white background, respectively [20].

2.4. Mechanical property characterization and finite element analysis

The micro-hardness and fracture toughness were determined by the indentation method using a Vickers micro-hardness tester (Model FV-700, Future- Tech, Tokyo, Japan) with a load of 98 N applied for 10 s on mirror-polished specimens. The indentation toughness was calculated according to the Anstis equation with an Young's modulus of 210 GPa [21]. In brief, Vickers indenter is used to make a hardness impression on a polished zirconia surface which would create a plastically deformed region underneath the indenter as well as cracks that emanate radially outwards from the indentation corners. The length of these cracks was measured and indentation fracture toughness is then computed following the equation by Anistis *et* al. (1981):

$$K_{ic} = 0.016 \cdot \frac{F}{c^{3/2}} \cdot \left(\frac{E}{HV}\right)^{1/2}$$

where *F* is force applied for the hardness test (N), *c* is the largest lateral extension of the crack (m), *E* is the modulus of elasticity of zirconia (GPa) and HV is Vickers hardness (GPa). For each ceramic grade, minimum 10 indentations were made.

The biaxial flexural strength was determined by piston-on-3-balls testing (P3B) on both sides mirror polished specimens according to the modified ISO standard 6872 (n = 20) [16]. Regarding the modification, plate-shaped specimens were used instead of discs in this work because they more closely matched the commercially available blocks for chairside processing. For validation of this modified ISO standard for plate-shaped specimens, Finite element analysis (FEA) was performed by using the commercial finite element code Abaqus V6.14. Different three-dimensional finite element

models (FEMs) were created in order to simulate square and circular specimens. In addition, 3 variations of these models were generated to simulate different loading conditions by modifying specimens' sizes (10, 12 and 15 mm) and the radius of the supporting circle ((1) 8mm for the 10mm specimens and (2) 10mm for the 12mm and 15mm specimens). For all simulations, a linear elastic material was defined with a Young's modulus equal to 210 GPa, a Poisson ratio equal to 0.25 [16] and a density of 6.05 kg/m^3 [22]. Piston loading was simulated by applying a compressive pressure load to the piston-loading surface (2 mm^2) located at the center of the specimens. Supporting balls were simulated by applying displacement constraints in the Z-direction at the specimen-ball contact areas. Three different loading conditions representing the load applied on the piston were simulated for each of the specimens (100, 1000 and 2000 MPa) based on the average expected strength of Y-TZP and Y-PSZ zirconia grades. The volume mesh is constructed using 10-node 3-D quadratic tetrahedral elements (C3D10) with a maximum element size of 200 µm. The element size was inside the asymptotic region of convergence and represented a good trade-off between numerical accuracy and computational cost for all cases. A sensitivity analysis was performed in order to determine the optimal element mesh size. The resulting 3D FEMs consist of a total of 151654 and 116098 elements for square and circular specimens, respectively.

All P3B tests were conducted on a universal machine (Instron 4467, Norwood, MA, USA) at a crosshead speed of 0.5 mm/min. After fracture, all fragments were carefully collected and their number was registered. The biaxial flexural strength of plate specimens was calculated as indicated in the ISO standard 6872 for disks, with the specimen radius replaced by half of the specimen side length [23] following the equations:

$$\sigma = -0.2387P(X - Y)/b^2 \tag{4}$$

$$X = (1 + \nu)\ln\left(\frac{r_2}{l}\right)^2 + \left[\frac{(1 - \nu)}{2}\right]\left(\frac{r_2}{l}\right)^2 \tag{5}$$

$$Y = (1 + \nu)\left[1 + \ln\left(\frac{r_1}{l}\right)^2\right] + (1 - \nu)\left(\frac{r_1}{l}\right)^2 \tag{6}$$

where σ is the maximum center tensile stress, P is the total load causing fracture (in N), v is the Poisson's ratio, r_1 is the radius of the support circle, r_2 is the radius of the loaded area, l is half of the specimen side length and b is the specimen thickness.

2.5. Statistical analysis and parameter correlations

Grain size, translucency and biaxial flexural strength of different zirconia grades were evaluated using one-way analysis of variance (ANOVA) followed by post-hoc Tukey or Games-Howell test for multiple

comparisons. Correlations between parameters of interest were tested using Pearson's correlation. All variables were dimensional except color, which was defined as a nominal (dihotomous) value. Correlations were considered statistically significant if $p<0.05$. All statistical analysis was performed using SPSS statistical software (SPSS, Version 20, Chicago, IL, USA).

3. RESULTS

3.1. Characterization of physical properties: microstructure, chemical and phase compositions

The chemical composition of the tested zirconia grades, as measured by XRF, is presented in Table 2. GC ST, GC HT and Lava Plus had rather similar compositions in terms of ZrO_2 (90 - 94 wt%) and Y_2O_3 content (5.3 - 5.6 wt%), characterizing them as 3 mol% yttria-stabilized zirconia (3Y-TZP). Katana HT and Katana ML contained 7.0 and 7.3 wt% of Y_2O_3, respectively, which corresponds to ≈4 mol%, thus representing 4Y-PSZ. The amount of Y_2O_3 in GC UHT and Katana STML was 9.5 wt% and 9.7 wt%, respectively, corresponding to a 5 mol% yttria-stabilized zirconia (5Y-PSZ). Finally, Katana UTML contained the highest Y_2O_3 (10.5 wt%) content, corresponding to 6 mol% yttria-stabilized zirconia (6Y-PSZ). Apart from a small amount of HfO_2 impurity, which is commonly found in all zirconia grades, GC ST, GC HT, Katana HT and Lava Plus contained a small amount of Al_2O_3, while Er_2O_3 could be found in Katana HT, Katana ML and Lava Plus. Additionally, Lava Plus revealed a small amount of Fe_2O_3.

XRD patterns reflecting the zirconia phase composition in each zirconia are shown in Fig. 1. All three 3Y-TZP (GC ST, GC HT and Lava Plus) zirconia grades displayed similar XRD patterns, while the two 4Y-PSZ zirconia grades Katana HT and Katana ML showed similarities among each other. In the same manner, the XRD patterns of the two 5Y-PSZ zirconia grades (GC UHT and Katana STML) and one 6Y-PSZ zirconia grades Katana UTML were similar. The peaks corresponding to tetragonal zirconia (*t*-ZrO_2) were clearly observed in the pattern of the 3Y-TZP zirconia grades whereas peaks representing the cubic phase (*c*-ZrO_2) were clearly detected in the 5Y-PSZ and 6Y-PSZ zirconia grades. Comparison of the XRD spectra between 70-80^o 2Θ showed that the *t'*-ZrO_2 phase doublet peaks in the 4Y-PSZ zirconia grades Katana ML and Katana HT overlapped more with the *c*-ZrO_2 peak. Monoclinic zirconia (*m*-ZrO_2) was not observed in any of the XRD patterns.

Rietveld analysis (Table 3) revealed the highest amount of *t*-ZrO_2 for the 3Y-TZP zirconia grades GC ST (81 ± 0.3wt%), GC HT (83±0.3 wt%) and Lava Plus (78±0.2 wt%). The amount of *t*-ZrO_2 for 4Y-PSZ zirconia grades Katana HT (55±5.5 wt%) and Katana ML (53±2.9 wt%) and the 5Y-PSZ Katana STML (47±2.1 wt%) was substantially lower, while the 6Y-PSZ zirconia grades Katana UTML (32±3.5 wt%) and GC UHT (31±0.8wt%) were characterized with the lowest amount of tetragonal phase. The amount of Y_2O_3 in the residual tetragonal phase was the highest for the 5Y-PSZ zirconia grades GC UHT (3.5 ± 0.04 mol%), Katana STML (4.2 ± 0.07 mol%) and the 6Y-PSZ zirconia grades Katana UTML (4.01 mol%), and substantially lower for the 3Y-TZP zirconia grades such as GC ST (2.6 ± 0 mol%), GC HT (2.6 ± 0.02 mol%), and Lava Plus (2.7±0.02 mol%). The tetragonal phase in the 4Y-PSZ zirconia grades Katana HT (2.4 ± 0.19 mol%) and Katana ML (2.3 ± 0.03 mol%) contained 2.4 mol% yttria. The tetragonality ($c/a\sqrt{2}$) in the residual tetragonal phase was expectedly higher in the 3Y-TZP zirconia grades GC ST (1.0154±0.00001), GC HT (1.0153±0.00004) and Lava Plus (1.0153±0.00002) as compared to the 5Y-PSZ zirconia grades GC UHT (1.0132±0.0001), Katana STML (1.0112±0.0002), Katana UTML

(1.0111±0.0004). However, the 4Y-PSZ zirconia grades Katana HT (1.0159 ± 0.0005) and Katana ML (1.0162 ± 0.0001), being 4Y-PSZ, have a tetragonal phase with a higher tetragonality than the investigated 3Y-TZPs.

The results of the SEM microstructural analysis are presented in Fig. 2. SEM showed a fully dense microstructure for all analyzed zirconia grades. The largest average grain size was observed in 6Y-PSZ Katana UTML (1.57±0.83 µm) and 5Y-PSZ Katana STML (1.14±0.6 µm). The average grain sizes of GC UHT, Katana HT and Katana ML were 0.43±0.21 µm, 0.4±0.24 µm, 0.36±0.2 µm, respectively. Furthermore, the 3Y-TZP zirconia grades GC HT (0.24±0.09 µm), GC ST (0.29±0.12 µm) and Lava Plus (0.29±0.11 µm) were revealed the smallest grain sizes. Moreover, the grain-size distribution histogram of Katana HT, Katana STML and Katana UTML showed a wide distribution tendency resulting in a bimodal grain-size distribution, while the other zirconia grades were presented with a unimodal grain-size distribution (Fig. 2).

3.2. Micro-Raman analysis

Representative µRaman spectra are presented in Fig. 3. The 3Y-TZP zirconia grades GC HT, GC ST and the 5Y-PSZ zirconia grades GC UHT, Katana STML and the 6Y-PSZ zirconia grade Katana UTML clearly revealed tetragonal peaks at 142 cm^{-1} and 256 cm^{-1}. On the other hand, the Er_2O_3 co-doped 3Y-TZP Lava Plus and 4Y-PSZ Katana ML and Katana HT were presented with a completely different spectrum exhibiting overwhelming peaks of high intensity in an unrecognizable pattern. Dual monoclinic phase bands at 178 and 190 cm^{-1} and a light tetragonal band at 384 cm^{-1} could not be detected in any of the tested zirconia grades.

3.3. Optical property characterization

The measured TP of the zirconia ceramics is presented in Fig. 4. The 6Y-PSZ and 5Y-PSZ zirconia grades revealed a significantly higher TP compared to the 4Y-PSZ and 3Y-TZP zirconia grades. The 5Y-PSZ zirconia grade GC UHT showed the highest TP, compared to the 6Y-PSZ zirconia grade Katana UTML and the other 5Y-PSZ zirconia grade Katana STML. At the same time, GC HT and Katana ML showed the highest TP among all analyzed 4Y-PSZ and 3Y-TZP zirconia grades. Moreover, Katana HT and Lava Plus showed a comparable translucency, while GC ST was the least translucent. The TP of the lithium disilicate glass-ceramic was significantly higher (TP=51.9) compared to TP of all zirconia ceramics.

3.4. Mechanical property characterization and finite element analysis

The Vickers hardness and fracture toughness results are presented in Table 4. The Vickers HV_{10} hardness of all zirconia grades was in the 13 GPa range. GC UHT (1377 kg/mm^2), GC HT (1373 kg/mm^2) and Katana STML (1345 kg/mm^2) showed the statistically highest Vickers hardness compared to the

other zirconia grades. On the other hand, the lowest hardness was observed for 4Y-TZP Katana ML and Katana HT (1326 and 1319 kg/mm^2, respectively). As expected, the fracture toughness was higher for the 3Y-TZP zirconia grades compared to the 4Y-PSZ and 5Y-PSZ zirconia grades. GC ST (4.2 MPa·m$^{1/2}$) revealed the statistically highest fracture toughness compared to the other 3Y-TZP zirconia grades, GC HT (3.8 MPa m$^{1/2}$) and Lava Plus (3.7 MPa m$^{1/2}$) and the 4Y-PSZ zirconia grades Katana HT (3.7 MPa m$^{1/2}$) and Katana ML (3.4 MPa m$^{1/2}$). The 5Y-PSZ GC UHT (2.6 MPa m$^{1/2}$) had a higher fracture toughness than Katana STML (2.4 MPa m$^{1/2}$) and the 6Y-PSZ zirconia grades Katana UTML (2.2 MPa m$^{1/2}$).

FEA results were presented in terms of maximum principal stress, which was evaluated at a central point located on the tensile surface of the specimens. Results for the different model dimensions and load parameters used for the different finite element simulations can be consulted in Table 5 for a representative loading condition of 1000 MPa applied at the loading piston area, while the stress distribution on the tensile specimen surface are presented in Fig. 5. As expected, the maximum tensile stress was registered in the center of the tensile surface for all specimens with a steady decrease towards the boundaries. A stress distribution in the form of a triple asymmetry can be observed in the projections of the supporting balls. Importantly, no differences in stress distribution could be observed between the discs and the plate-shaped specimens for the three different specimen configurations simulated (Fig. 5). This is also the case under other typical failure load conditions ranging between 100 and 2000 MPa (supplementary Table 1). The differences between the FEA predictions and the analytical values using Eq. 4-6, for all simulated cases varied between 0.2 % and 2.3 % (Table 5). These small differences suggest that Eq. 4-6 can be used to calculate the biaxial flexural strength for both disc and plate geometries.

The biaxial strength results including the average flexural strength, characteristic strength (σ_0) [95% CI] and Weibull plots were presented in Table 4 and Fig. 6. All 3Y-TZP zirconia grades, except Lava Plus, showed a significantly higher biaxial strength compared to the Y-PSZ zirconia grades. The highest strength was measured for GC ST (1556±264 MPa) and GC HT (1439±146 MPa), which was significantly stronger than the 4Y-PSZ zirconia grades Katana HT (952±112 MPa) and Katana ML (928±87 MPa). The 3Y-TZP zirconia grades Lava Plus (773±107 MPa) had a comparable biaxial strength as the 5Y-PSZ zirconia grades Katana STML (702±127 MPa) and GC UHT (680±163 MPa). Katana UTML (606±907 MPa) revealed the lowest strength. The Weibull modulus of the 3Y-TZP zirconia grades, GC HT (m=11.7) and Katana ML (m=10.8), was the highest of all zirconia grades, followed by Katana HT (m=9.8), Lava HT (m=8) and GC ST (m=7). Katana UTML (m=6.5), Katana STML (m=6.3) and GC UHT (m=4.7) were least reliable.

3.5. Parameter correlations

Correlations between different parameters were presented in Fig. 7 and the supplement Table 2. For the flexural strength, a negative correlation was observed with the *c*-ZrO_2 phase content and the total Y_2O_3 content, while a positive correlation was observed between flexural strength and fracture toughness. Additionally, a positive correlation of the cubic ZrO_2-phase content was observed with the Y_2O_3 content and translucency, but the cubic ZrO_2-phase content negatively correlated with the fracture toughness. At the same time a higher overall Y_2O_3 content was also negatively related to the *t*-ZrO_2 phase tetragonality and the fracture toughness. Tetragonality negatively correlated to translucency (TP) and fracture toughness. Interestingly, the average grain size was not significantly related to any parameter analyzed, while the sintering temperature only negatively correlated with the hardness. No correlation between coloring and toughness, and flexural strength was observed, while the addition of coloring agents statistically negatively correlated with the hardness of the zirconia grade.

4. DISCUSSION

Together with the growing popularity of zirconia ceramics in dentistry, a wide range of commercial zirconia grades are being introduced on the market every year. For this reason, a thorough characterization of currently representative materials was warranted. In the present study, a broad range of commercially available multilayer and monolayer dental zirconia ceramics was investigated clearly reflecting different microstructures and physical features resulting in different optical and mechanical properties. Moreover, a strong correlation was found between the parameters that influence the microstructure, mechanical properties and translucency. Therefore, our starting hypothesis stating that there is no relationship between specific physical, mechanical and optical properties of both monolayer and multilayer zirconia grades, can be rejected.

In accordance with the previous studies [17,24], chemical characterization of GC ST, GC HT and Lava Plus revealed the lowest Y_2O_3 content, which is characteristic for 3Y-TZP. Moreover, Katana HT and ML were characterized as 4Y-PSZ, while the even higher amount of Y_2O_3 in Katana STML and GC UHT is characteristic for 5Y-PSZ. Katana UTML contained ≈6 mol% yttria, which is characteristic for 6Y-PSZ. In the 3Y-TZP and 4Y-PSZ zirconia grades such as GC ST, GC HT and Lava Plus and Katana ML, respectively, a small amount of Al_2O_3 was detected (Table 2). The role of the sintering aid of Al_2O_3 in Y-TZP systems has already extensively been studied. It has been shown that a low alumina amount (<0.25 wt%) influences the microstructure and retards the hydrothermal degradation of Y-TZP without compromising its mechanical properties [25]. However, Al_2O_3 can drastically decrease the translucency of zirconia ceramics [25–27], in agreement with the lowest TP observed in this study for GC ST that revealed the highest Al_2O_3 amount (0.36 wt%). As expected, a small amount of HfO_2 (<5 wt%) was identified in all investigated zirconia grades. Hf is known as a common unintentional zirconia contaminant, which is difficult to separate from the ore during ZrO_2 production due to their similar chemistry [28] and stability of their complete solid solutions [29]. Natural teeth are not white as pure zirconia and intentionally adding coloring dopants is a quite known method to improve their optical appearance. Er_2O_3 and Fe_2O_3 coloring dopants were detected in Katana ML/HT and Lava Plus, respectively. While Er_2O_3 is light violet, addition of Fe_2O_3 into zirconia gives it a yellow–brown color without diminishing its flexural strength and toughness [30]. This relationship was confirmed by the parameter-correlation analysis (Fig. 7). The coloring of zirconia negatively affected hardness but interestingly did not have any effect on the material translucency (TP). It is important to mention that multilayered materials can be expected to not have the same chemical composition throughout the specimen as the darker dentin layers will contain higher pigment content compared to the lighter enamel layers. However, due to the relative large size of the XRF sampling beam, it was impossible to evaluate chemical composition layer by layer. Thus, all XRF analysis was done by sampling the middle of the plate specimen.

Since practically all properties of Y-TZP zirconia grades depend on their microstructure and ZrO_2-phase stabilization, a quantitative determination of the phase content is of high importance. Even though there are different ways to quantify the phase content, X-ray diffraction (XRD) and µRaman spectroscopy are considered to be the most powerful non-destructive methods. In general, a higher yttria content will yield a higher amount of cubic phase in the zirconia ceramic [31]. Specifically, this relationship can clearly be explained by the ZrO_2-Y_2O_3 phase diagram (Fig. 8), which contains all tested zirconia grades since they were all characterized by a binary tetragonal-cubic (T-C) phase composition. The phase-structure differences between the investigated materials were also reflected in the tetragonality of the *t*-ZrO_2 phase (Table 3). Clearly, 3Y-TZP showed a higher tetragonality compared to the 5Y-PSZ and 6Y-PSZ zirconia grades. In accordance with previous research, a lower Y_2O_3 content will result in a higher tetragonality and the concomitant lower *t*-ZrO_2-phase stability will positively influence the *t*-ZrO_2-phase transformability and the material toughness [31]. Interestingly, 4Y-TZP materials Katana ML and Katana HT revealed the highest tetragonality. This could be attributed to their bimodal microstructure, in which Y^{3+} was more enriched in the cubic phase leading to a decreased Y^{3+} content in the remaining tetragonal grains [32].

The phase composition of the tested zirconia grades quantified by XRD, was partially confirmed by µRaman spectroscopy. In contrast to XRD, µRaman is known as a powerful tool with a high spatial resolution (≈4 µm in this work) [33], which allows identification of different ZrO_2 phases (mostly monoclinic and tetragonal) in small areas of the analyzed material. While both tetragonal and monoclinic ZrO_2-crystal phases produce strong and sharp Raman peaks, which could be easily quantified by their intensity [34], quantification of cubic phase ZrO_2 is much more difficult due to the high "background" profile and a specific broad cubic peak between 530 and 670 cm^{-1} that overlaps with the monoclinic and tetragonal band [35]. Non-colored yttria-stabilised zirconia, such as GC HT, GC ST and GC UHT, and the highly translucent multilayered Katana STML and Katana UTML have a typical µRaman spectrum with well-formed tetragonal peaks at 142 cm^{-1} and 256 cm^{-1}, and additional peaks at 316 cm^{-1} and 460 cm^{-1}. Interestingly, Katana HT, Katana ML and Lava Plus gave rise to a wide µRaman spectrum characterized by particularly intensive overwhelming peaks, which is most likely related to the various coloring dopants and fluorescence enhancers that are often added to their composition (see Fig. 3). From Table 2, the only compound that could be related with this phenomenon is the Er_2O_3-coloring agent, which was only detected in the three specific zirconia grades, Katana HT, Katana ML and Lava Plus. To the best of our knowledge, this has not yet been reported, and it is assumed that specific dopants and fluorescent enhancers might be Raman active, generating their own Raman spectrum that overwhelms the characteristic ZrO_2 peaks. This hypothesis finds support in the fact that each repetitive measurement resulted in a higher peak intensities compared to the previous one (data

not shown), as well as it is corroborated by the fact that Fe_2O_3-doped zirconia reveals a typical zirconia μRaman spectrum [9].

SEM enabled to reveal the grain size of the different zirconia grades. While the grain size of the 3Y-TZP (GC ST, GC HT and Lava Plus) zirconia grades was rather comparable, the 4Y-PSZ (Katana HT and Katana ML) zirconia grades had significantly larger grains (Fig. 2). Additionally, the grain size distribution of Katana HT and Katana STML clearly showed a bimodal grain-size distribution. It should be kept in mind that all 3-6 mol% yttria doped zirconia ceramics are mixtures of tetragonal and cubic ZrO_2 phases (see Fig. 8) [31]. Therefore, the larger grains observed in 4Y-PSZ Katana HT and STML are most likely cubic ZrO_2-phase grains [36].

In accordance with previously published research regarding the influence of the above discussed microstructural and phase features on the translucency [37], our correlation analysis confirmed that a higher Y_2O_3 and concomitant cubic ZrO_2-phase content increased the material translucency (Fig. 7). Therefore, 5Y-PSZ and 6Y-PSZ zirconia grades showed higher translucency compared to their 4Y-PSZ and 3Y-TZP counterparts (Fig. 4), but these translucency levels are still substantially lower than that of the highly translucent lithium disilicate glass ceramics. A further improvement in optical properties of zirconia is required to become competitive with feldspatic porcelain and glass ceramics, being crucial for their justified presence on the dental market. A significant difference in translucency of the 3Y-TZP zirconia grades was found and could be explained by the specific microstructure and chemical composition of each individual zirconia grade. GC ST (ST=standard translucency) is a conventional first-generation dental zirconia containing >0.25 wt% Al_2O_3, has a lower translucency than GC HT (high translucency) despite their rather comparable microstructure (phase composition, tetragonality, Y_2O_3 content, grain size). However, the presence of a relatively high amount of Al_2O_3-sintering aid in GC ST (0.31 wt% compared to 0.17 wt% in GC HT) leads to the formation of secondary phase alumina particles during sintering that serve as light scattering points reducing the zirconia translucency. On the other hand, Lava Plus (second-generation dental zirconia) has a rather similar microstructure as GC HT, including a comparable Al_2O_3 content, but conversely shows a significantly lower translucency [37]. This could be explained by the presence of the specific metal oxides such as Er_2O_3 and Fe_2O_3 ,which are used for pre-coloring of the zirconia powder that gives the zirconia grade a more natural appearance after sintering but at the same time a diminished translucency [10]. Most likely for the same reason, the non-colored 5Y-PSZ zirconia grade GC UHT showed a higher translucency compared to the colored 5Y-PSZ zirconia grade Katana STML and the 6Y-PSZ zirconia grade Katana UTML, while the translucency of the colored 4Y-PSZ zirconia grades Katana ML and Katana HT was in the range of that of the 3Y-TZP zirconia grades.

3Y-TZP zirconia grades, except from Lava Plus (which was in the range of the 5Y-PSZ zirconia grades), had a substantially higher characteristic flexural strength compared to the other zirconia grades (Table 4, Fig. 6). This flexural strength was also comparable with characteristic flexural strength reported in previous studies [17]. The relationship between the microstructure and mechanical properties of Y-TZP ceramics has already vastly been studied [38] and is confirmed by the correlation analysis (Fig. 7). The total Y_2O_3 content negatively correlated with the tetragonal phase content, flexural strength and toughness. This was expected as a higher tetragonality indicates a lower *t*-ZrO_2-phase stability, which will further reflect in the high tetragonal phase transformability and subsequently higher fracture toughness based on transformation toughening [32,39]. Moreover, a high tetragonality (c-axis to a-axis lattice parameter ratio) also indicates a predominately tetragonal crystal structure, which is at the same time known for a low translucency (*high opacity*) due to the light scattering birefringence at the grain boundaries [32]. On the other hand, the presence of pigments in zirconia only negatively correlated with the micro-hardness. Although this relationship has already been reported in various studies [40], consensus is not reached in literature as some researchers reported no effect of coloring on the mechanical properties of zirconia ceramics [12]. Although statistically significant differences in hardness between particular zirconia grades were observed (Table 4), their hardness was in the range of fully dense zirconia ceramics and in accordance with previously reported studies [17,41], while coloring indeed had no effect on flexural strength and toughness.

It is noteworthy to mention that the biaxial flexural strength of the commercial zirconia grades was measured in a piston-on-3-balls test (P3B) according to ISO standard 6872 [16], but using plate-shaped specimens instead of disk-shaped specimens. This P3B test has already been proven suitable for testing small brittle disks. Many researchers have tried to validate this P3B test for different specimen sizes and shapes [42,43]. In particular, commercial zirconia is usually supplied in the pre-sintered state either in the form of relatively small blocks (indicated solely for single tooth restorations such as inlays, partial crowns and single full crowns) or of larger disks (indicated for fabrication of multi-teeth FDPs) of various thickness that could be easily cut into small rectangular shaped specimens. Thus, P3B testing of plate-shaped specimens has several advantages among which time saving for specimen reshaping and more importantly offering the possibility to test all layers of the newly introduced multilayered zirconia ceramic. However, one should bear in mind that the stress generation during P3B testing is highly related to the geometrical details of the set-up and the specimen shape. A validation of the biaxial flexural strength equation commonly used for disc shaped specimens is needed when using other shapes or sizes. For this reason, FEA was employed to evaluate stress distribution and to accurately analyze the stress field. In this study, particular zirconia plate-shaped specimens of different length (10, 12 and 15 mm) were analyzed (Table 5). No difference in stress-distribution pattern was observed between plate-shaped specimens and disks, with the maximum tensile stress concentrated

in the middle of the specimen with a gradually decrease towards the specimen borders, as shown in Fig. 5.

According to the Griffith equation, material strength is strongly influenced by the intrinsic fracture toughness as well as microstructural features, while also by the presence of flaws and defects or more precisely the flaw distribution [44]. No zirconia ceramic is perfectly homogeneous and during/after zirconia production and processing, a discrete number population of flaws (defects), such as residual pores, inclusions, microcracks, and surface scratches, will be present in the final material structure [45]. Therefore, according to the generally accepted "weakest link theory", the largest (critical) flaw within the regions under tensile stress will play a crucial role in the failure of a zirconia object [44]. Using proper statistical analysis, such as Weibull analysis, will take into consideration the presence of flaw distributions, is crucial for characterizing the mechanical reliability and failure probability of zirconia ceramics into consideration [46]. The current results agree with previous research, which have reported *m* values between 5 and 11 for Y-TZP materials [47,48]. In general, the Weibull distribution plots revealed the lowest shape (*m*) values for 5Y-PSZ and 6Y-PSZ materials in comparison to other zirconia grades (see Fig. 6). The 4Y-PSZ zirconia grade Katana HT/ML showed rather high shape values, which are comparable with those of 3Y-TZP zirconia grades. Increased reliability of 3Y-TZP compared to 5Y-PSZ is attributed to the increased fracture resistance due to the *t-m* transformability and lower sensitivity to cracks [36]. High shape values or Weibull moduli, characteristic for 3Y-TZP, are mechanically favorable as they imply a narrower strength window for failure, i.e. higher mechanical reliability. However, the 3Y-TZP zirconia grade GC ST, characterized with the highest biaxial flexural strength, showed a relatively low shape value (*m*), indicating modest mechanical reliability.

5. CONCLUSION

This research revisits the microstructural and phase characteristics of current commercial zirconia ceramics, giving rise to comprehensive correlations between chemical composition, microstructure, mechanical and optical properties. Additionally, specific concerns and challenges in the methodology design have been covered. µRaman spectroscopy can provide additional information regarding the presence of specific coloring agents, such as Er_2O_3 doping-related fluorescent effects. FEA confirmed the validity of the equations to calculate the biaxial flexural strength when piston-on-3-balls (P3B) testing plate-shape zirconia specimens instead of discs. All tested commercial dental zirconia grades had a Vickers hardness of ~13 GPa. Irrespective of the zirconia grade, the 3Y-TZP and 4Y-PSZ zirconia grades showed the highest fracture toughness and flexural strength compared to the 5Y-PSZ and 6Y-PSZ zirconia grades. Except from GC HT, the 3Y-TZP materials showed a lower mechanical reliability (Weibull modulus) than 4Y-PSZ but were more reliable than 5Y-PSZ and 6Y-PSZ ceramics. As expected, the 6Y-PSZ and 5Y-PSZ zirconia grades had a higher translucency than the opaquer 4Y-PSZ and 3Y-TZP zirconia grades, but these values were still substantially lower than for lithium disilicate glass-ceramic.

ACKNOWLEDGEMENTS

This study was funded by the KU Leuven research project C24/17/084 and the Research Foundation - Flanders (FWO-Vlaanderen) grant G0B2618N. F. Zhang and M. Cóndor thank FWO-Vlaanderen for her post-doctoral fellowship 12S8418N and 12ZR120N. M. Inokoshi would like to thank the JSPS Grant-in-Aid for Scientific Research (C) JP19K10241. We would like to thank the manufacturers for providing the commercial zirconia ceramics. We thank Mr. Nicolas Courtois (Anthogyr, France) for kindly providing the piston-on-3-balls test jig. We thank Prof. Marleen Peumans (KU Leuven) for the translucency measurements. We thank Drs. Hengyi Liu for the specimen preparation and XRD analysis.

REFERENCES

[1] Garvie RC, Hannink RH, Pascoe RT. Ceramic steel? Nature 1975. https://doi.org/10.1038/258703a0.

[2] Tabatabaian F. Color Aspect of Monolithic Zirconia Restorations: A Review of the Literature. J Prosthodont 2018:1–12. https://doi.org/10.1111/jopr.12906.

[3] Zhang Y, Lawn BR. Novel Zirconia Materials in Dentistry. J Dent Res 2018;97:140–7. https://doi.org/10.1177/0022034517737483.

[4] Kontonasaki E, Giasimakopoulos P, Rigos AE. Strength and aging resistance of monolithic zirconia: an update to current knowledge. Jpn Dent Sci Rev 2020;56:1–23. https://doi.org/10.1016/j.jdsr.2019.09.002.

[5] Hurle K, Werbach K. A Revised Relationship Between Fracture Toughness and Y2O3 Content in Modern Dental Zirconias 2021:1–23.

[6] A. D, G. L. Shading vita YZ substructures: Influence on value and chroma, Part I. Int J Comput Dent 2004.

[7] Devigus A, Lombardi G. Shading Vita In-ceram YZ substructures: influence on value and chroma, part II. Int J Comput Dent 2004.

[8] Shah K, Holloway JA, Denry IL. Effect of Coloring with Various Metal Oxides on the Microstructure, Color, and Flexural Strength of 3Y-TZP. J Biomed Mater Res - Part B Appl Biomater 2008. https://doi.org/10.1002/jbm.b.31107.

[9] Ban S, Suzuki T, Yoshihara K, Sasaki K, Kawai T, Kono H. Effect of coloring on mechanical properties of dental zirconia. J Med Biol Eng 2014;34:24–9. https://doi.org/10.5405/jmbe.1425.

[10] Tuncel I, Eroglu E, Sari T, Usumez A. The effect of coloring liquids on the translucency of zirconia framework 2013:10–3.

[11] Nakamura K, Harada A, Ono M, Shibasaki H, Kanno T, Niwano Y, et al. Effect of low-temperature degradation on the mechanical and microstructural properties of tooth-colored 3Y-TZP ceramics. J Mech Behav Biomed Mater 2016;53:301–11. https://doi.org/10.1016/j.jmbbm.2015.08.031.

[12] Sedda M, Vichi A, Carrabba M, Capperucci A, Louca C, Ferrari M. Influence of coloring procedure on flexural resistance of zirconia blocks. J Prosthet Dent 2015;114:98–102. https://doi.org/10.1016/j.prosdent.2015.02.001.

[13] Lümkemann N, Pfefferle R, Jerman E, Sener B, Stawarczyk B. Translucency, flexural strength, fracture toughness, fracture load of 3-unit FDPs, Martens hardness parameter and grain size of 3Y-TZP materials. Dent Mater 2020. https://doi.org/10.1016/j.dental.2020.03.027.

[14] Zhang F, Inokoshi M, Batuk M, Hadermann J, Naert I, Van Meerbeek B, et al. Strength,

toughness and aging stability of highly-translucent Y-TZP ceramics for dental restorations. Dent Mater 2016;32:e327–37. https://doi.org/10.1016/j.dental.2016.09.025.

[15] Dahl P, Kaus I, Zhao Z, Johnsson M, Nygren M, Wiik K, et al. Densification and properties of zirconia prepared by three different sintering techniques. Ceram Int 2007;33:1603–10. https://doi.org/10.1016/j.ceramint.2006.07.005.

[16] ISO6872:2015. Dentistry — Ceramic materials. Geneva:International Organization for Standardization (ISO); 2015. p. 1-28

[17] Cokic SM, Vleugels J, Van Meerbeek B, Camargo B, Willems E, Li M, et al. Mechanical properties, aging stability and translucency of speed-sintered zirconia for chairside restorations. Dent Mater 2020. https://doi.org/10.1016/j.dental.2020.04.026.

[18] Yamashita I, Tsukuma K. Phase Separation and Hydrothermal Degradation of 3 mol% Y2O3-ZrO2 Ceramics. J Ceram Soc Japan 2005;533:530–3.

[19] Gibson IR, Irvine JTS. Qualitative X-ray Diffraction Analysis of Metastable Tetragonal (t') Zirconia. J Am Ceram Soc 2001;84:615–8. https://doi.org/10.1111/j.1151-2916.2001.tb00708.x.

[20] Nogueira AD, Della Bona A. The effect of a coupling medium on color and translucency of CAD-CAM ceramics. J Dent 2013;41:e18–23. https://doi.org/10.1016/j.jdent.2013.02.005.

[21] Anstis GR, Chantikul P, Lawn BR, Marshall DB. A Critical Evaluation of Indentation Techniques for Measuring Fracture Toughness: I, Direct Crack Measurements. J Am Ceram Soc 1981;64:533–8. https://doi.org/10.1111/j.1151-2916.1981.tb10320.x.

[22] Inokoshi M, Zhang F, De Munck J, Minakuchi S, Naert I, Vleugels J, et al. Influence of sintering conditions on low-temperature degradation of dental zirconia. Dent Mater 2014;30:669–78. https://doi.org/10.1016/j.dental.2014.03.005.

[23] Da J, Fraga S, Vogel GF, May LG. Influence of the geometry of ceramic specimens on biaxial flexural strength: experimental testing and finite element analysis. Ceramica 2018;64:120–5. https://doi.org/10.1590/0366-69132018643692287.

[24] Inokoshi M, Shimizu H, Nozaki K, Takagaki T, Yoshihara K, Nagaoka N, et al. Crystallographic and morphological analysis of sandblasted highly translucent dental zirconia. Dent Mater 2018;34:508–18. https://doi.org/10.1016/j.dental.2017.12.008.

[25] Zhang F, Vanmeensel K, Inokoshi M, Batuk M, Hadermann J, Van Meerbeek B, et al. Critical influence of alumina content on the low temperature degradation of 2-3mol% yttria-stabilized TZP for dental restorations. J Eur Ceram Soc 2015;35:741–50. https://doi.org/10.1016/j.jeurceramsoc.2014.09.018.

[26] Carrabba M, Keeling AJ, Aziz A, Vichi A, Fabian Fonzar R, Wood D, et al. Translucent zirconia in the ceramic scenario for monolithic restorations: A flexural strength and translucency

comparison test. J Dent 2017;60:70–6. https://doi.org/10.1016/j.jdent.2017.03.002.

[27] Jiang L, Liao Y, Li W, Wan Q, Zhao Y. Influence of alumina addition on the optical property of zirconia/alumina composite dental ceramics. J Wuhan Univ Technol Mater Sci Ed 2011;26:690–5. https://doi.org/10.1007/s11595-011-0294-1.

[28] Banda R, Lee HY, Lee MS. Separation of Zr and Hf from strong hydrochloric acid solution by solvent extraction with TEHA. J Radioanal Nucl Chem 2013;295:1537–43. https://doi.org/10.1007/s10967-012-1941-5.

[29] Ruh R, Garrett HJ, Domagala RF, Tallan NM. The System Zirconia-Hafnia. J Am Ceram Soc 1968. https://doi.org/10.1111/j.1151-2916.1968.tb11822.x.

[30] Holz L, Macias J, Vitorino N, Fernandes AJS, Costa FM, Almeida MM. Effect of Fe2O3 doping on colour and mechanical properties of Y-TZP ceramics. Ceram Int 2018. https://doi.org/10.1016/j.ceramint.2018.06.273.

[31] Krogstad JA, Lepple M, Gao Y, Lipkin DM, Levi CG. Effect of yttria content on the zirconia unit cell parameters. J Am Ceram Soc 2011;94:4548–55. https://doi.org/10.1111/j.1551-2916.2011.04862.x.

[32] Zhang F, Van Meerbeek B, Vleugels J. Importance of tetragonal phase in high-translucent partially stabilized zirconia for dental restorations. Dent Mater 2020:1–10. https://doi.org/10.1016/j.dental.2020.01.017.

[33] Muñoz Tabares JA, Anglada MJ. Quantitative analysis of monoclinic phase in 3Y-TZP by raman spectroscopy. J Am Ceram Soc 2010;93:1790–5. https://doi.org/10.1111/j.1551-2916.2010.03635.x.

[34] Pezzotti G, Porporati AA. Raman spectroscopic analysis of phase-transformation and stress patterns in zirconia hip joints. J Biomed Opt 2004;9:372. https://doi.org/10.1117/1.1647547.

[35] Kontoyannis CG, Orkoula M. Quantitative determination of the cubic, tetragonal and monoclinic phases in partially stabilized zirconias by Raman spectroscopy. J Mater Sci 1994;29:5316–20. https://doi.org/10.1007/BF01171541.

[36] Zhang F, Reveron H, Spies BC, Van Meerbeek B, Chevalier J. Trade-off between fracture resistance and translucency of zirconia and lithium-disilicate glass ceramics for monolithic restorations. Acta Biomater 2019;91:24–34. https://doi.org/10.1016/j.actbio.2019.04.043.

[37] Zhang Y. Making yttria-stabilized tetragonal zirconia translucent. Dent Mater 2014;30:1195–203. https://doi.org/10.1016/j.dental.2014.08.375.

[38] Trunec M. Effect of grain size on mechanical properties of 3Y-TZP ceramics. Ceram - Silikaty 2008;52:165–71.

[39] Hannink RHJ, Kelly PM, Muddle BC. Transformation Toughening in Zirconia-Containing Ceramics. J Am Ceram Soc 2004;83:461–87. https://doi.org/10.1111/j.1151-

2916.2000.tb01221.x.

[40] Donmez MB, Olcay EO, Demirel M. Influence of coloring liquid immersion on flexural strength, Vickers hardness, and color of zirconia. J Prosthet Dent 2021:1–6. https://doi.org/10.1016/j.prosdent.2020.11.020.

[41] Turp V, Tuncelli B, Sen D, Goller G. Evaluation of hardness and fracture toughness, coupled with microstructural analysis, of zirconia ceramics stored in environments with different pH values. Dent Mater J 2012. https://doi.org/10.4012/dmj.2012-005.

[42] Wendler M, Belli R, Petschelt A, Mevec D, Harrer W, Lube T, et al. Chairside CAD/CAM materials. Part 2: Flexural strength testing. Dent Mater 2017;33:99–109. https://doi.org/10.1016/j.dental.2016.10.008.

[43] Danzer R, Supancic P, Harrer W, Lube T, Borger A. Biaxial strength testing on mini specimens. Fract Nano Eng Mater Struct - Proc 16th Eur Conf Fract 2006;i:589–90. https://doi.org/10.1007/1-4020-4972-2_292.

[44] Gonzaga CC, Cesar PF, Miranda WG, Yoshimura HN. Slow crack growth and reliability of dental ceramics. Dent Mater 2011;27:394–406. https://doi.org/10.1016/j.dental.2010.10.025.

[45] Hadjicharalambous C, Prymak O, Loza K, Buyakov A, Kulkov S, Chatzinikolaidou M. Effect of porosity of alumina and zirconia ceramics toward pre-osteoblast response. Front Bioeng Biotechnol 2015;3. https://doi.org/10.3389/fbioe.2015.00175.

[46] Quinn JB, Quinn GD. A practical and systematic review of Weibull statistics for reporting strengths of dental materials. Dent Mater 2010;26:135–47. https://doi.org/10.1016/j.dental.2009.09.006.

[47] Pereira GKR, Guilardi LF, Dapieve KS, Kleverlaan CJ, Rippe MP, Felipe L. Journal of the Mechanical Behavior of Biomedical Materials Mechanical reliability , fatigue strength and survival analysis of new polycrystalline translucent zirconia ceramics for monolithic restorations. J Mech Behav Biomed Mater 2018;85:57–65. https://doi.org/10.1016/j.jmbbm.2018.05.029.

[48] Inokoshi M, Shimizubata M, Nozaki K, Takagaki T, Yoshihara K, Minakuchi S, et al. Impact of sandblasting on the flexural strength of highly translucent zirconia. J Mech Behav Biomed Mater 2021;115:104268. https://doi.org/10.1016/j.jmbbm.2020.104268.

TABLES

Table 1: Commercial zirconia grades studied with the category and sintering process mentioned as defined by the manufacturer.

Commercial name	Manufacturer	Category	Heating rate (peak temperature)	Peak temperature (dwell time)	Cooling rate (temperature where next cooling phase starts)
GC ST	GC	Standard translucency, Monolayer-bleach	8.3 °C/min (1000 °C) 1.6 °C/min (1450 °C)	1450 °C (2h)	7.5 °C/min (1000 °C)
GC HT	GC	High translucency, Monolayer-bleach			
GC UHT	GC	Ultra-High translucency, Monolayer-bleach			
Lava Plus	3M Oral Care, Seefeld, Germany	High translucency, monolayer – A2	20 °C/min (800 °C) 10 °C/min (1450 °C)	1450 °C (2h)	15 °C/min (800 °C) 20 °C/min (250 °C)
Katana HT	Kuraray Noritake, Tokyo, Japan	High translucency, monolayer – A2	10 °C/min (1500 °C)	1500 °C (2h)	10 °C/min
Katana ML	Kuraray Noritake, Tokyo, Japan	Multilayer* – A2			
Katana STML	Kuraray Noritake, Tokyo, Japan	Super Translucent, Multilayered* – A2	10 °C/min (1550 °C)	1550 °C (2h)	10 °C/min
Katana UTML	Kuraray Noritake, Tokyo, Japan	Ultra Translucent, Multilayered* – A2			

* four layers: enamel (35%), two transition layers (15% each) and dentin layer (35%); information taken from the manufacturer.

Table 2. The elemental composition of the commercial zirconia grades, as analyzed by XRF

Composition (wt%)	GC ST	GC HT	GC UHT	Katana HT	Katana ML	Katana STML	Katana UTML	Lava Plus
ZrO_2	92.6	93.5	89.7	91.2	90.6	88.0	87.7	90.9
Y_2O_3	5.3±0.5	5.5±0.4	9.5±0.5	7.0±0.2	7.3±0.2	9.7±0.7	10.5±0.1	5.5±0.1
HfO_2	1.47	1.2	1.1	1.1	1.3	1.5	1.4	1.4
Al_2O_3	0.35	0.11			0.16			0.16
Er_2O_3				0.19	0.12			0.46
Fe_2O_3								0.10
	3Y-TZP	3Y-TZP	5Y-PSZ	4Y-PSZ	4Y-PSZ	5Y-PSZ	6Y-PSZ	3Y-TZP
Generation (appearance)	1st	2nd	3rd	3rd (colored)	3rd (colored, multilayer)	3rd (colored, multilayer)	3rd (colored, multilayer)	3rd (colored, multilayer)

Table 3. Phase composition and lattice parameters, as obtained by XRD pattern Rietveld analysis.

		GC ST	GC HT	GC UHT	Katana HT	Katana ML	Katana STML	Katana UTML	Lava Plus
Tetragonal	**Fraction (%)**	81.0±0.3	83±0.3	31±0.8	55±5.5	53±2.9	47±2.1	32.16±	78±0.2
	c (Å)	5.18±0.0002	5.18±0.0009	5.17±0.0001	5.18±0.0008	5.18±0.0001	5.17±0.0007	5.17±0.0029	5.18±0.0003
	a (Å)	3.61±0.0001	3.61±0.0005	3.61±0.0003	3.60±0.0012	3.60±0.0003	3.61±0.0002	3.62±0.0011	3.61±0.0003
	c/av2	1.0154	1.0153	1.0132	1.0159	1.0162	1.0112	1.0111	1.0153
	Y_2O_3(mol%)	2.62±0	2.6±0.02	3.5±0.04	2.4±0.19	2.3±0.03	4.2±0.07	4.01±0.14	2.7±0.02
Cubic	**fraction (%)**	19±0.3	17±0.3	69±0.8	44±5.5	44±2.9	53±2.1	64±3.61	22±0.2
	***c* (Å)**	5.14±0.0003	5.14±0.0004	5.13±0.0001	5.13±0.0001	5.13±0.0003	5.17±0.0007	5.14±0.0015	5.13±0.0002

Table 4. Vickers hardness, indentation toughness, mean biaxial flexural strength, Weibull modulus and characteristic strength of the tested zirconia ceramics

	Hardness (kg/mm^2)	Toughness ($MPa\ m^{1/2}$)	Biaxial flexural strength (MPa)	Weibull analysis	
	Mean±SD	Mean±SD	Mean±SD	m	σ_0 (MPa)
GC ST	1341±22^{ad}	4.2±0.2^{a}	1556±264^{a}	7	1623
GC HT	1373±18^{bc}	3.7±0.2^{b}	1439±146^{a}	12	1459
GC UHT	1377±17^{c}	2.6±0.1^{c}	680±163d^{cd}	5	728
Katana HT	1319±19^{a}	3.7±0.1^{b}	952±112^{b}	10	986
Katana ML	1326±15^{a}	3.4±0.2^{d}	928±87^{b}	11	938
Katana STML	1345±23^{abcd}	2.4±0.2^{ce}	702±127^{cd}	6	737
Katana UTML	1340±19^{a}	2.2±0.1^{e}	606±907^{d}	7	632
Lava Plus	1333±13^{a}	3.7±0.1^{b}	773±107^{c}	8	800

Table 5. FEA simulation after 1000 MPa simulated pressure (load) on the piston.

	Disks			Plates		
Radius/specimen side length (mm)	10	12	15	10	12	15
Surface (mm^2)	79	113	177	100	144	225
FE simulated stress (MPa)	946.6	1050.1	1034.04	964.8	1053.6	1044.2
Analytical value (MPa)	952.1	1051.9	1021.2	952.1	1051.9	1021.2
Error (%)	0.6	0.2	-2.3	-1.3	-0.2	-1.2

Supplementary Table 1: FEA simulations after 100 MPa and 2000 MPa simulated pressure (load) on the piston:

		Disks			Plates		
	Radius/specimen side length (mm)	10	12	15	10	12	15
	Surface (mm^2)	79	113	177	100	144	225
100 MPa	FE simulated stress (MPa)	94.7	105	103.4	96.5	105.4	104.4
	Analytical value (MPa)	95.2	105.2	102.1	95.2	105.2	102.1
	Error (%)	0.6	0.2	-2.2	-1.3	-0.2	-1.3
2000 MPa	FE simulated stress (MPa)	1879.5	2100.29	2068.1	1929.5	2086.2	2088.4
	Analytical value (MPa)	1904.3	2103.7	2042.4	1904.3	2103.7	2042.4
	Error (%)	1.3	0.2	-2.3	-1.3	0.8	-1.3

Supplementary Table 2: Pearson correlation analysis between different tested parameters.

	Cubic cont.	Y_2O_3	Tetragonality	Grain size	Translucency	Hardness	F. strength	Toughness	Sintering T	Color
Cubic cont.	X	**0.837****	-0.353	0.270	**0.752***	0.107	**-0.715***	**-0.713***	0.345	0.196
Y_2O_3	**0.837****	X	**-0.749***	0.385	**0.778***	0.066	**-0.824***	**-0.937****	0.564	0.404
Tetragonality	-0.353	**-0.749***	X	-0.554	-0.645	-0.178	0.587	**0.874****	-0.384	-0.242
Grain size	0.270	0.385	-0.554	X	0.298	-0.286	-0.447	-0.516	0.577	0.455
Translucency	**0.752***	**0.778***	-0.645	0.298	X	0.617	-0.604	**-0.869****	0.053	-0.114
Hardness	0.107	0.066	-0.178	-0.286	0.617	X	0.127	-0.244	-0.692	**-.767***
F. strength	**-0.715***	**-0.824***	0.587	-0.447	-0.604	0.127	X	**0.806***	-0.599	-0.629
Toughness	**-0.713***	**-0.937****	**0.874****	-0.516	**-0.869****	-0.244	**0.806***	X	-0.450	-0.303
Sintering T	0.345	0.564	-0.384	0.577	0.053	-0.692	-0.599	-0.450	X	**.932****
Color	0.196	0.404	-0.242	0.455	-0.114	**-0.767***	-0.629	-0.303	**0.932****	x

FIGURES:

Figure 1.

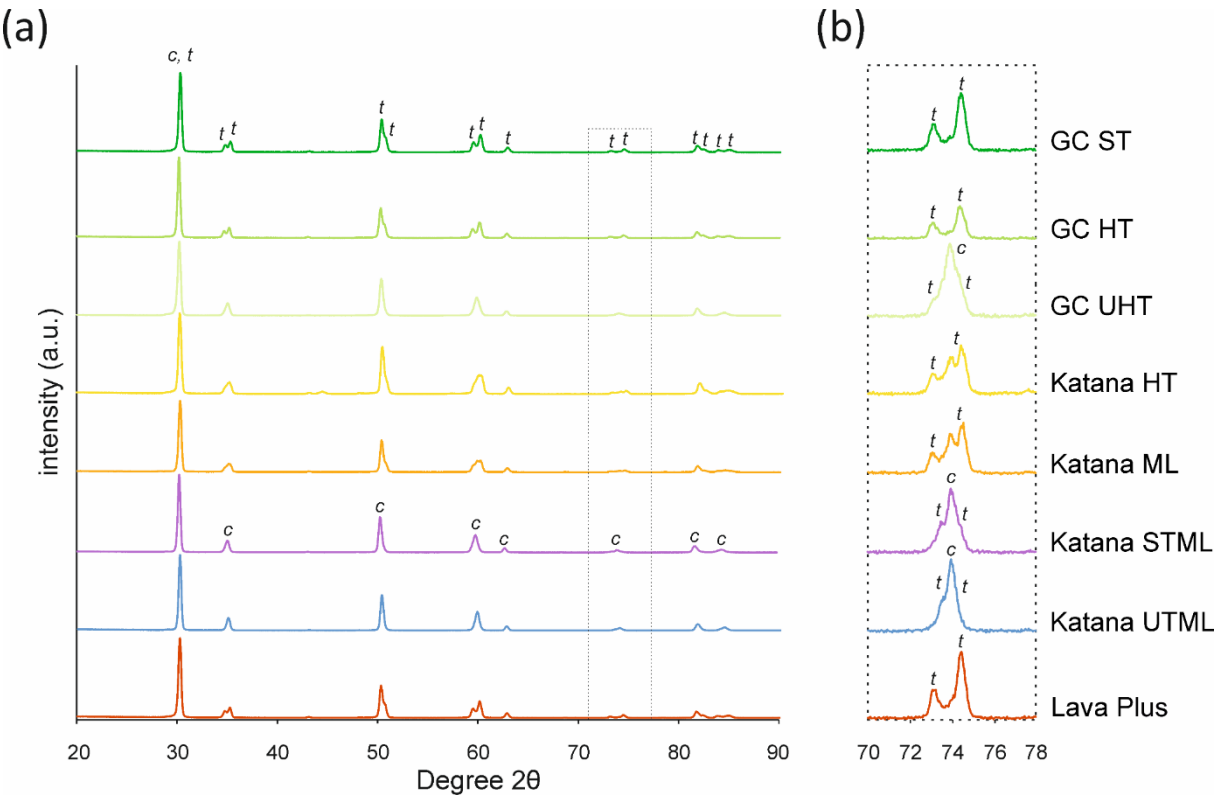

Figure 2.

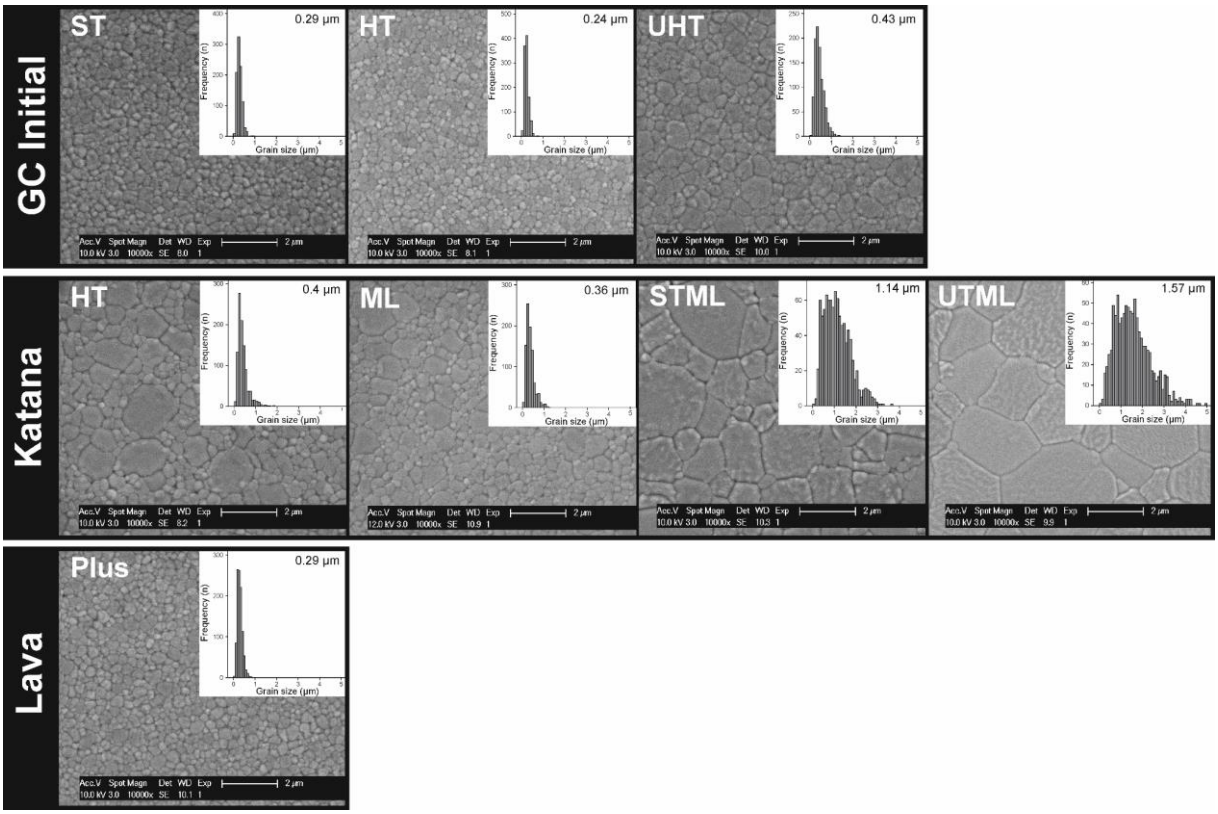
GC Initial
ST
0.29 µm
HT
0.24 µm
UHT
0.43 µm
Katana
HT
0.4 µm
ML
0.36 µm
STML
1.14 µm
UTML
1.57 µm
Lava
Plus
0.29 µm
Frequency (n)
Grain size (µm)

Figure 3.

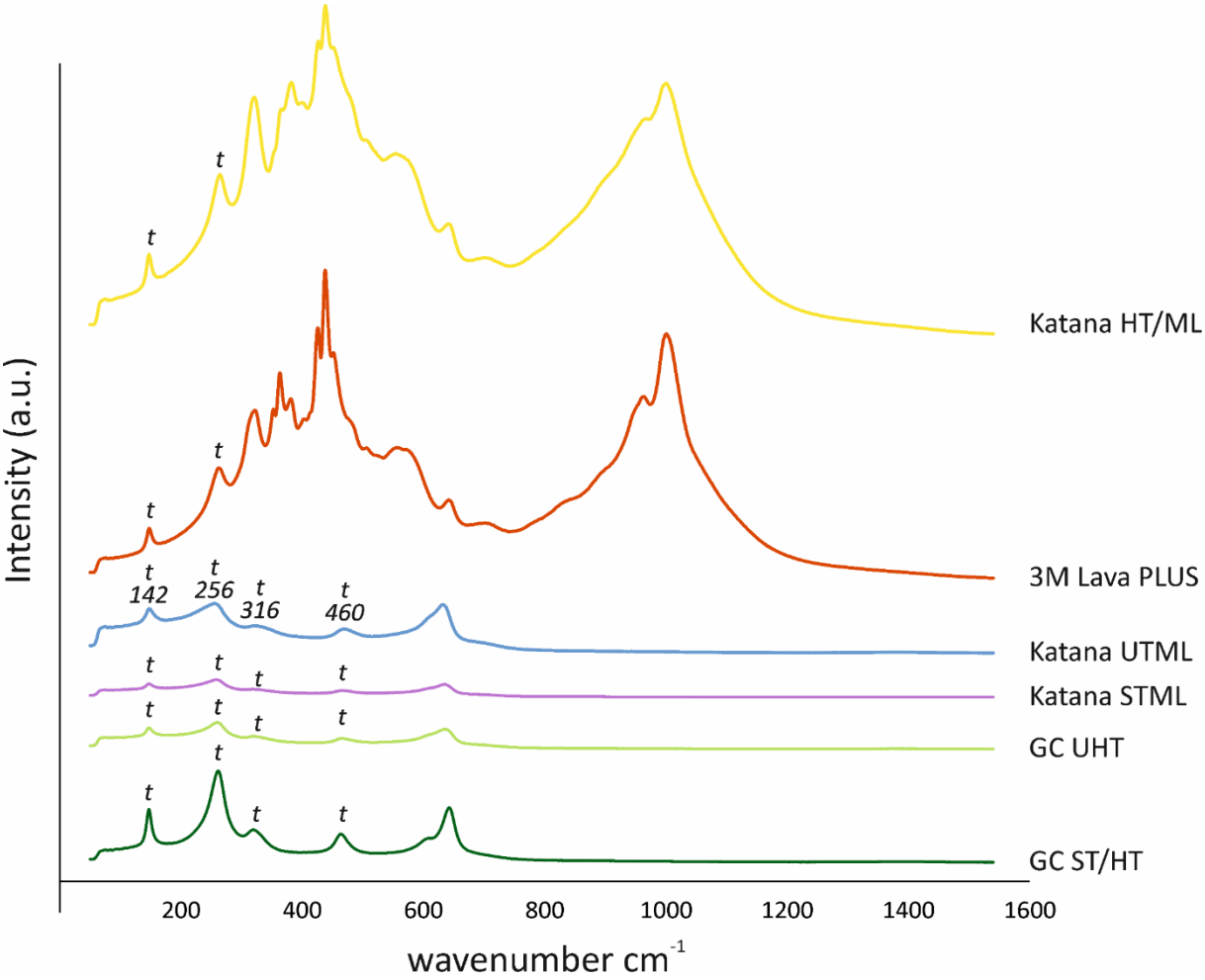
Intensity (a.u.)
wavenumber cm-1
200
400
600
800
1000
1200
1400
1600
Katana HT/ML
3M Lava PLUS
Katana UTML
Katana STML
GC UHT
GC ST/HT
t
142
256
316
460

Figure 4.

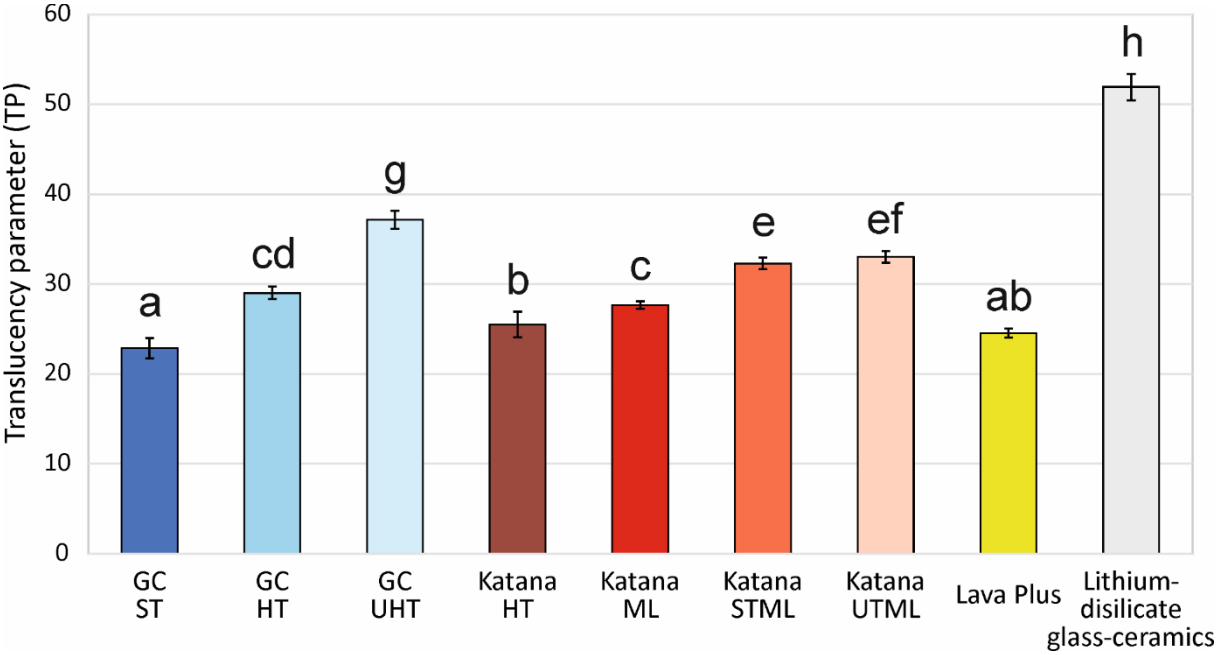
Translucency parameter (TP)
60
50
40
30
20
10
0
a
cd
g
b
c
e
ef
ab
h
GC ST
GC HT
GC UHT
Katana HT
Katana ML
Katana STML
Katana UTML
Lava Plus
Lithium-disilicate glass-ceramics

Figure 5.

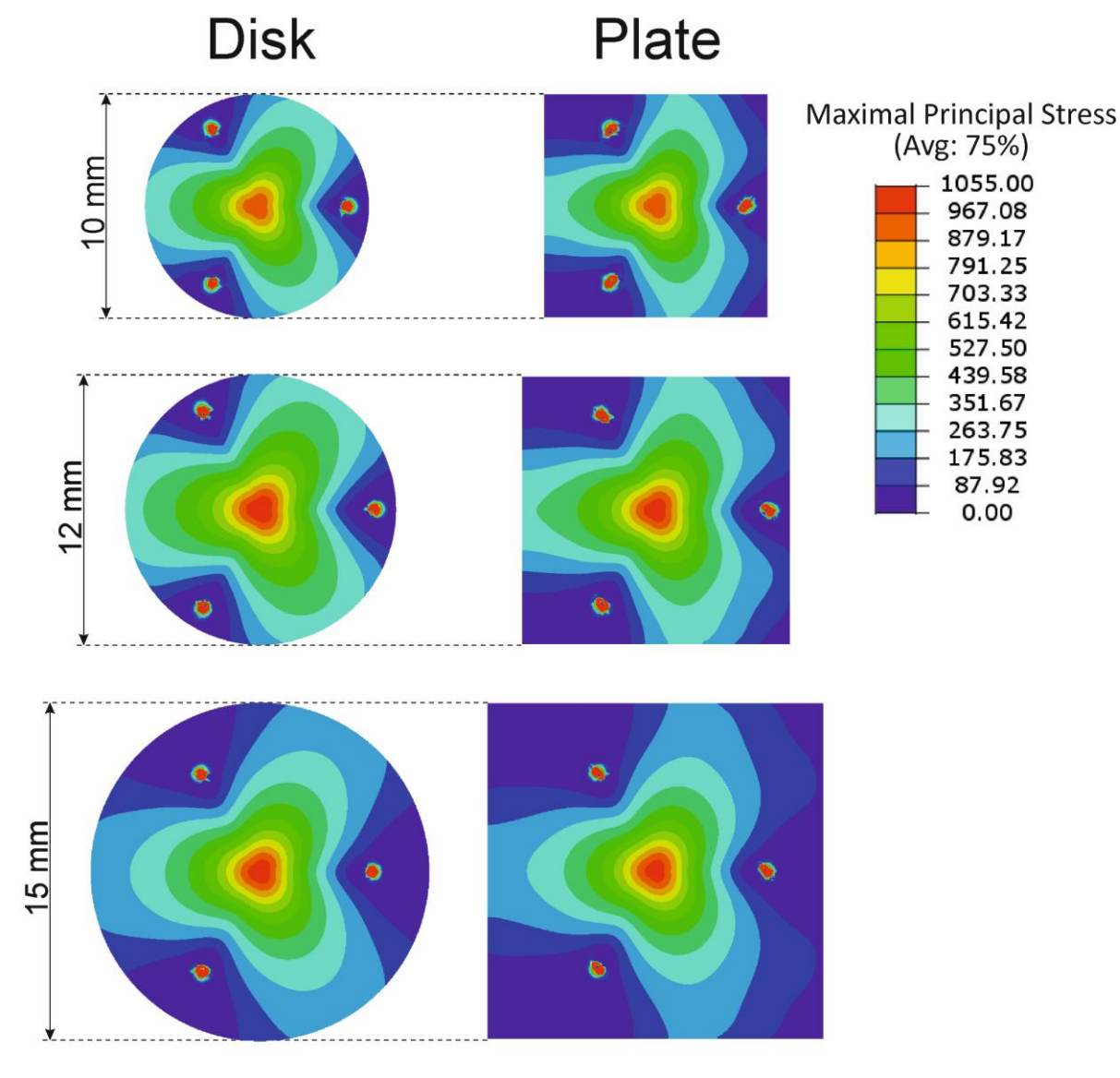
Disk
Plate
10 mm
12 mm
15 mm
Maximal Principal Stress
(Avg: 75%)
1055.00
967.08
879.17
791.25
703.33
615.42
527.50
439.58
351.67
263.75
175.83
87.92
0.00

Figure 6.

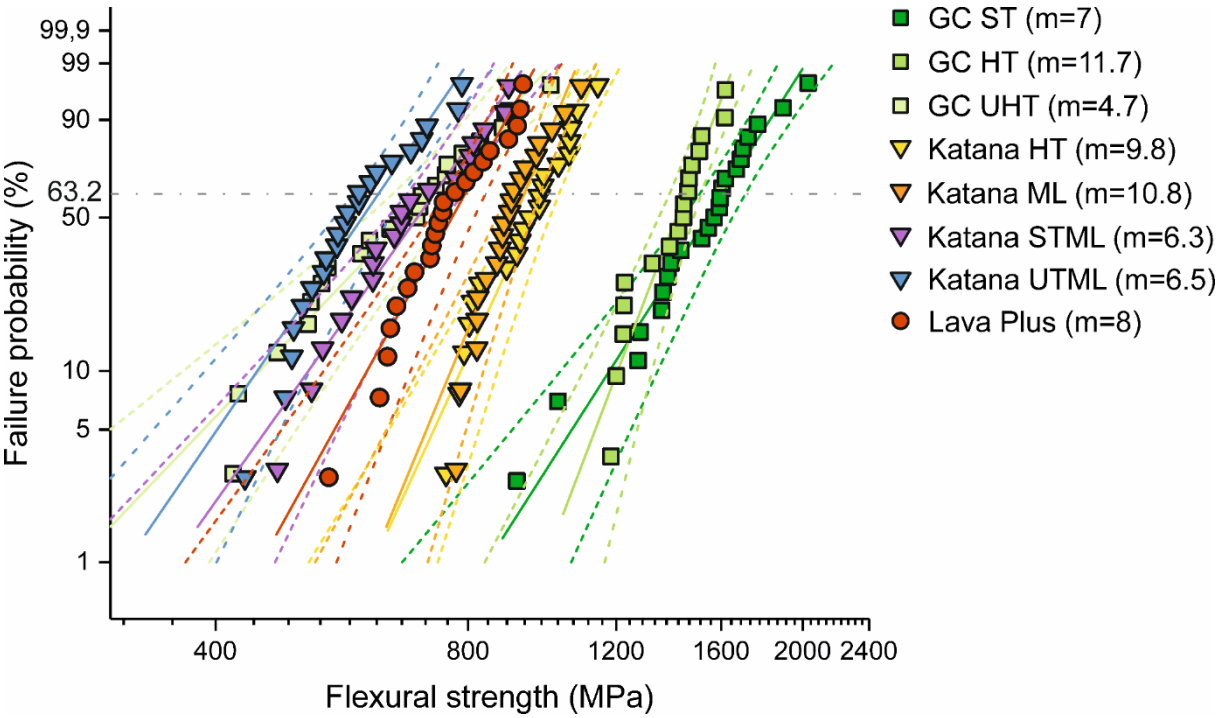
99,9
99
90
63,2
50
10
5
1
Failure probability (%)
400
800
1200
1600
2000
2400
Flexural strength (MPa)
GC ST (m=7)
GC HT (m=11.7)
GC UHT (m=4.7)
Katana HT (m=9.8)
Katana ML (m=10.8)
Katana STML (m=6.3)
Katana UTML (m=6.5)
Lava Plus (m=8)

Figure 7.

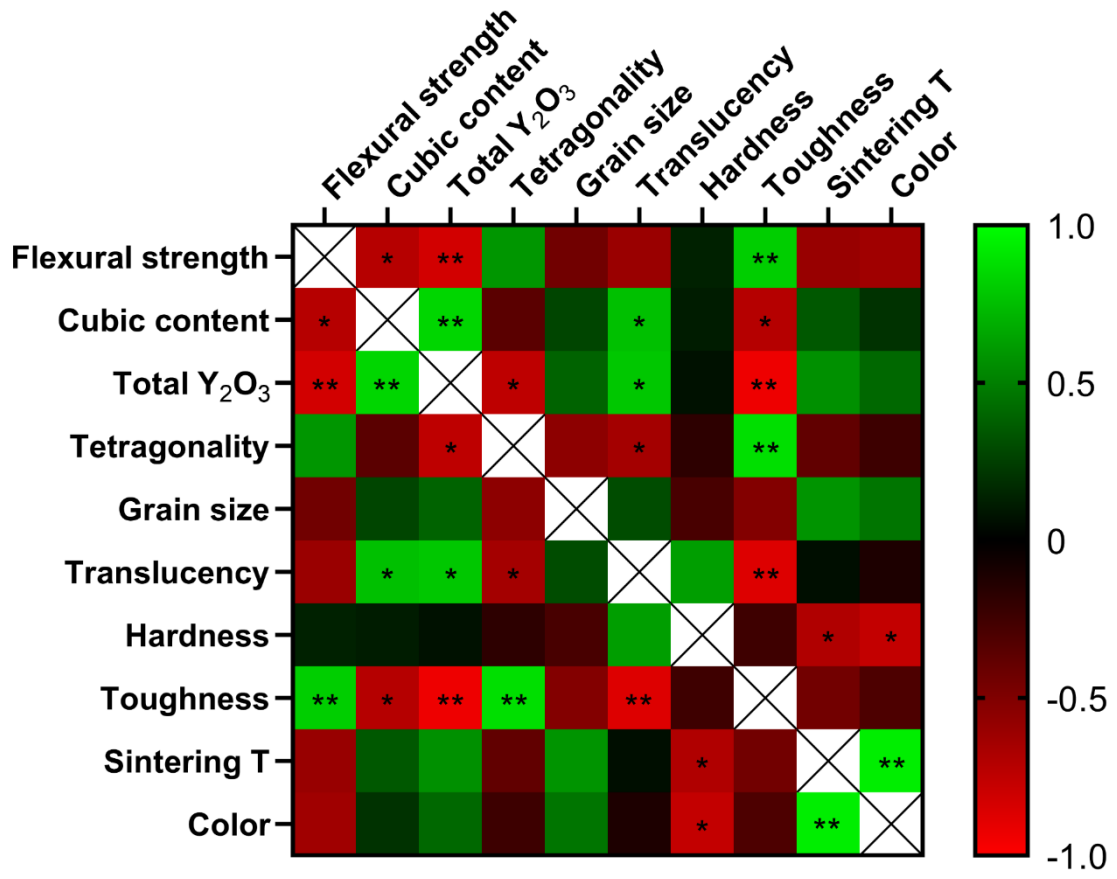
Flexural strength
Cubic content
Total Y_2O_3
Tetragonality
Grain size
Translucency
Hardness
Toughness
Sintering T
Color
1.0
0.5
0
-0.5
-1.0

Figure 8.

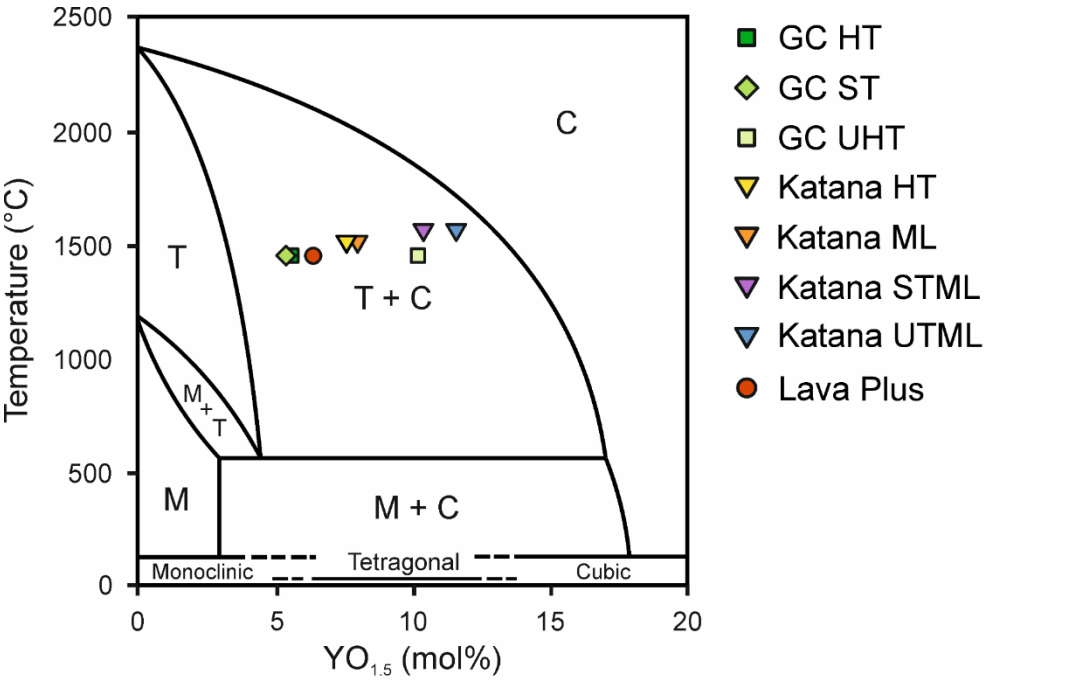
2500
2000
1500
1000
500
0
Temperature (°C)
0
5
10
15
20
YO1.5 (mol%)
C
T
T + C
M + T
M
M + C
Monoclinic
Tetragonal
Cubic
GC HT
GC ST
GC UHT
Katana HT
Katana ML
Katana STML
Katana UTML
Lava Plus

FIGURE CAPTIONS:

Fig. 1: Representative XRD patterns of the sintered and polished zirconia grades. (a) The characteristic peaks of cubic and tetragonal zirconia are indexed with *c* and *t*. respectively. (b) Expanded view of the 70-78° 2Θ range.

Fig. 2: Representative SEM photo micrographs of the commercial 3Y-TZP, 4Y-PSZ, 5Y-PSZ and 6Y-PSZ zirconia grades.

Fig. 3: Representative micro-Raman spectra of the analyzed zirconia grades. GC ST/HT, GC UHT and Katana STML.

Fig. 4: Translucency of the commercial zirconia grades analyzed. The letter annotation represents the significant difference between the tested zirconia-ceramic specimens at the significance level ($p<0.05$).

Fig. 5: Simulated stress distribution on the tensile surface, supported by three balls of different size disk and plate-square specimens for a representative 1000 MPa pressure (load) condition. A triple symmetry stress distribution is generated on the tensile side, which is independent of the specimen shape (disc or plate) and size.

Fig. 6: Biaxial flexural strength of commercial zirconia grades tested. Weibull plot with 95% confidence bands. The horizontal dotted line represents the Weibull characteristic strength (failure probability of 63.2%).

Fig. 7: Pearson correlation analysis between the different factors tested. Differences were considered statistically significant if $p<0.05$.

Fig. 8: Phase equilibrium diagram of tested commercial zirconia grades, as represented by their overall Y_2O_3 content and sintering temperature.